COMPDYN 2011
III ECCOMAS Thematic Conference on
Computational Methods in Structural Dynamics and Earthquake Engineering
M. Papadrakakis, M. Fragiadakis, V. Plevris (eds.)
Corfu, Greece, 25–28 May 2011

MULTISCALE RKPM FORMULATION FOR MODELING PENETRATION OF AN ULTRA HIGH-STRENGTH CONCRETE MATERIAL

M. J. Roth[1], J. S. Chen[2], T. R. Slawson[1], R. N. Boone[1], X. Ren[2], S. W. Chi[2], C. H. Lee[2], and P. C. Guan[2]

[1] U.S. Army Engineer Research and Development Center
3909 Halls Ferry Road, Vicksburg, MS, 39180
e-mail: {michael.j.roth, thomas.r.slawson, nicholas.boone}@usace.army.mil

[2] Department of Civil and Environmental Engineering
University of California, Los Angeles
P.O. Box 159310, Los Angeles, CA, 90095-1593
jschen@seas.ucla.edu, chishengwei@ucla.edu, rxd1981@gmail.com, ch.lee@ucla.edu,
paichen@ntou.edu.tw

Keywords: RKPM, multiscale, microcrack, damage model, ultra high-strength concrete, penetration

Abstract. *Impact and penetration events involve complex response phenomena such as damage and fragmentation, which present particular challenges to numerical methods like the finite element method. Further, the commonly used phenomenological damage law gives no direct consideration to the evolution of continuum-scale damage with respect to microcrack formation and growth within the substructure. In this work, we introduced the reproducing kernel particle method (RKPM) to impact and penetration problems, and a hierarchical multiscale modeling technique under the framework of RKPM is proposed. A multiscale damage model is developed based on homogenization of a cracked microscopic cell, which is termed the microcrack-informed damage model (MIDM). Bridging between scales is accomplished by a novel energy equivalence approach. Application of the MIDM to a specific ultra high-strength concrete material is discussed, and results from the analysis of a benchmark penetration problem are presented.*

1 INTRODUCTION

Impact and penetration events represent a class of complex physical problems that are of significant interest in both military and commercial applications. These can generally be considered as "strong dynamics" problems, which exhibit high strain rates (10^3-10^7 s^{-1} for ballistic events [1]), large velocity gradients, and fast-evolving strong and weak discontinuities that lead to extensive material and structural damage and fragmentation. The level of complexity is further enhanced when considered in the context of concrete structures due to concrete's brittle response and highly heterogeneous microstructure. In particular, material fragmentation poses a significant challenge to structured-mesh-based methods such as the finite element method (FEM). Due to extensive material deformation and separation, techniques such as element erosion have been commonly implemented to circumvent instabilities resulting from excessive mesh distortion. However, erosion is not consistent with the physical event, and subsequently precludes accurate modeling of certain effects such as debris generation from the impact zone. Therefore new meshfree methods, which do not exhibit the structured-mesh dependency of FEM, can provide significantly enhanced capabilities for impact and penetration modeling.

Accurate mathematical description of material softening, degradation and failure processes plays a dominant role in the accuracy of penetration modeling. The typical phenomenological description of damage evolution at the continuum scale lacks a direct link to the underlying microstructure processes. Damage processes in brittle solids such as concrete are driven by the distribution of microcracks and their evolution, and thus the applicability of continuum damage models requires further enhancement. In this work, a multiscale approach is introduced to link the continuum damage evolution to substructure crack propagation based on an energy bridging approach. This multiscale model is developed under the framework of the meshfree reproducing kernel particle method to model concrete penetration. The resulting multiscale damage evolution model has been termed the microcrack-informed damage model (MIDM) [7]. An ultra high-strength concrete developed by the U.S. Army Engineer Research and Development Center (ERDC) was adopted as a material for use in the formulation development.

The purpose of this paper is to provide an overview of the RKPM formulation for penetration modeling and discuss the development of the microcrack-informed damage model. Organization of the paper is as follows. Section 2 provides an overview of RKPM utilizing a semi-Lagrangian formulation, and Section 3 discusses the microcrack-informed damage model formulation. Section 4 presents implementation of the MIDM into a concrete constitutive model developed for penetration, and a benchmark penetration problem is analyzed in Section 5. Concluding remarks are given in Section 6.

2 REPRODUCING KERNEL PARTICLE METHOD

The reproducing kernel particle method (RKPM) [2,3] is a meshfree method in which the approximation and domain discretization of a partial differential equation are accomplished by a set of nodes related through domains of influence, also known as support zones. The support zones are non-conforming, which alleviates many of the structured-mesh dependent problems associated with FEM. This minimization of mesh dependency provides a distinct advantage when applying RKPM to impact and penetration problems, where very large material deformation and/or separation are common. A typical RKPM discretization is

shown in Figure 1a, where the non-conforming support zone of node **I** is highlighted. The corresponding shape function over the i^{th} node's compact support is shown in Figure 1b.

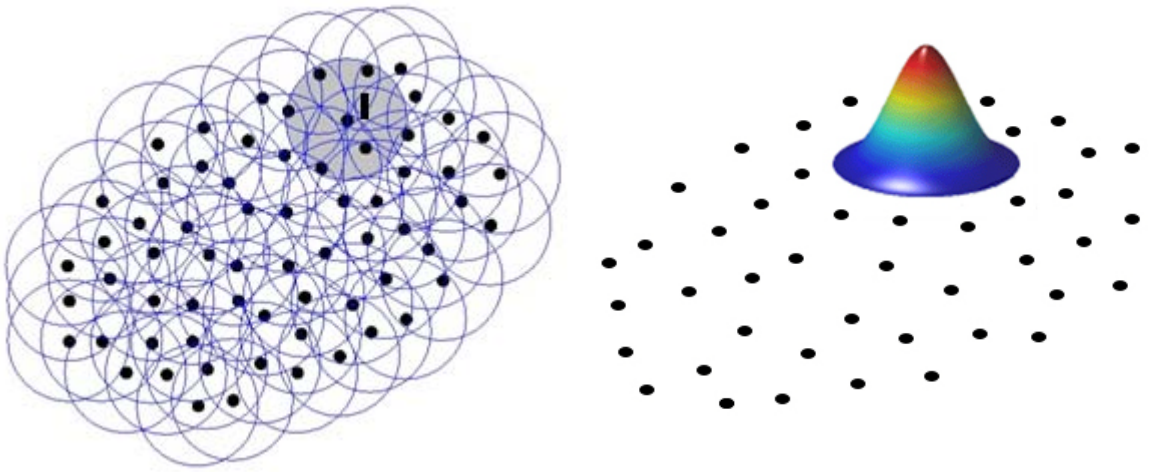

(a) **(b)**

Figure 1. a) Non-conforming, compact support of i^{th} node, b) RKPM shape function for i^{th} node

2.1 Semi-Lagrangian RKPM

In the following discussions, we use the general *d*-dimensional notation, where $x^{\alpha} = x_1^{\alpha_1} \cdots x_d^{\alpha_d}$ and $|\alpha| = \sum_{i=1}^{d} \alpha_i$. For the subject of interest, we consider the reproducing kernel (RK) approximation of degree *p* of a displacement field, $\boldsymbol{u}$, denoted by $\boldsymbol{u}^h$ as

$$\boldsymbol{u}^h(\boldsymbol{x}) = \sum_{I=1}^{n} C(\boldsymbol{x}; \boldsymbol{x} - \boldsymbol{x}_I)\Phi_a(\boldsymbol{x} - \boldsymbol{x}_I)\boldsymbol{d}_I \equiv \sum_{I=1}^{n} \Psi_I(\boldsymbol{x})\, \boldsymbol{d}_I \tag{1}$$

where $\Psi_I(\boldsymbol{x})$ is the RK shape function, $\Phi_a(\boldsymbol{x} - \boldsymbol{x}_I)$ is a scalar-valued kernel function with compact support (for example, the cubic B-spline function), $\boldsymbol{d}_I$ are the RK approximation coefficients for displacement, and $C(\boldsymbol{x}; \boldsymbol{x} - \boldsymbol{x}_I)$ is the correction function expressed as

$$C(\boldsymbol{x}; \boldsymbol{x} - \boldsymbol{x}_I) = \boldsymbol{H}^T(\boldsymbol{x} - \boldsymbol{x}_I)\, \boldsymbol{b}(\boldsymbol{x}) \tag{2}$$

where $\boldsymbol{H}^T(\boldsymbol{x} - \boldsymbol{x}_I) = \{(\boldsymbol{x} - \boldsymbol{x}_I)^{\alpha}\}_{|\alpha| \le p}$ is a vector of monomial basis functions of degree *p*, and $\boldsymbol{b}^T(\boldsymbol{x}) = \{b_{\alpha}(\boldsymbol{x})\}_{|\alpha| \le p}$ is a vector of unknown coefficients to be solved by using the reproducing conditions

$$\sum_{I=1}^{n} \Psi_I(\boldsymbol{x})\, \boldsymbol{x}_I^{\alpha} = \boldsymbol{x}^{\alpha} \quad \alpha \le p \tag{3}$$

Utilizing the reproducing condition of (3), $\boldsymbol{b}(\boldsymbol{x})$ may be solved by

$$\boldsymbol{b}(\boldsymbol{x}) = \boldsymbol{M}^{-1}(\boldsymbol{x})\boldsymbol{H}(\boldsymbol{0}) \tag{4}$$

where $\boldsymbol{H}^T(\boldsymbol{0}) = [1, 0, 0 \ldots 0]$ and ***M(x)*** is a moment matrix defined as

$$\boldsymbol{M}(\boldsymbol{x}) = \sum_{I=1}^{n} \boldsymbol{H}(\boldsymbol{x} - \boldsymbol{x}_I)\boldsymbol{H}^T(\boldsymbol{x} - \boldsymbol{x}_I)\Phi_a(\boldsymbol{x} - \boldsymbol{x}_I) \tag{5}$$

Utilizing (2) and (4) in conjunction with (1), the complete RK approximation is given as

$$\boldsymbol{u}^h(\boldsymbol{x}) = \sum_{I=1}^{n} \boldsymbol{H}^T(\boldsymbol{0})\boldsymbol{M}^{-1}(\boldsymbol{x})\boldsymbol{H}(\boldsymbol{x} - \boldsymbol{x}_I)\Phi_a(\boldsymbol{x} - \boldsymbol{x}_I)\boldsymbol{d}_I \tag{6}$$

The RK approximation may be formulated in a Lagrangian [4] or semi-Lagrangian [5] form, based on update of the support zone for each node. In the Lagrangian formulation, the support of each node is defined in the initial configuration, as shown in Figure 2a. This determines a "list" of neighboring nodes contained within the i^{th} node's support zone. The

definition of nodal support is not modified during the calculation, so that the same nodes remain in the i^{th} node's support throughout. As a result, the support zones deform with the material, as shown in Figure 2b. However, the Lagrangian formulation and discretization of conservation laws breaks down when mapping between the initial and current configurations is no longer one-to-one. This occurs under conditions such as new free surface formation (i.e. material separation) or free-surface closure, which commonly exist in damage processes of geomaterials.

Similar to the Lagrangian formulation, in the semi-Lagrangian formulation the nodal support conditions are first defined in the initial configuration. However, in the semi-Lagrangian formulation the neighboring node list is incrementally updated based on the material deformation and readjustment of support size. As a result, in the semi-Lagrangian formulation nodes are allowed to move in and out of the i^{th} node's support. Consequently, the nodal support zones do not deform with the material, as shown in Figure 2c. This property is necessitated in impact and penetration problems due to material separation and moving contact surfaces [6].

According to [5], the semi-Lagrangian RK shape function is expressed as

$$\Psi_I^{SL}(\boldsymbol{x}) = \boldsymbol{H}^T\big(\boldsymbol{x} - \boldsymbol{x}(\boldsymbol{X}_I, t)\big)\boldsymbol{b}(\boldsymbol{x})\Phi_a(\boldsymbol{x} - \boldsymbol{x}(\boldsymbol{X}_I, t)) \tag{7}$$

where $\boldsymbol{x} - \boldsymbol{x}(\boldsymbol{X}_I, t)$ indicates distance measurements taken in the current configuration and $\Psi_I^{SL}(\boldsymbol{x})$ is used to denote the semi-Lagrangian shape function. Let the velocity approximation be expressed by the semi-Lagrangian RK shape function

$$\dot{\boldsymbol{u}}^h(\boldsymbol{x}, t) = \boldsymbol{v}^h(\boldsymbol{x}, t) = \sum_{I=1}^{n} \Psi_I^{SL}(\boldsymbol{x})\, \boldsymbol{v}_I(t) \tag{8}$$

where $\dot{\boldsymbol{u}}^h$ is the time derivative of $\boldsymbol{u}^h$ and $\boldsymbol{v}_I(t)$ are the RK approximation coefficients for velocity. Taking the time derivative of (8) gives the approximation of acceleration as

$$\ddot{\boldsymbol{u}}^h(\boldsymbol{x}, t) = \dot{\boldsymbol{v}}^h(\boldsymbol{x}, t) = \sum_{I=1}^{n}[\Psi_I^{SL}(\boldsymbol{x})\dot{\boldsymbol{v}}_I(t) + \Psi_I^{*}(\boldsymbol{x})\boldsymbol{v}_I(t)] \tag{9}$$

where

$$\Psi_I^{*}(\boldsymbol{x}) = C\big(\boldsymbol{x}; \boldsymbol{x} - \boldsymbol{x}(\boldsymbol{X}_I, t)\big)\dot{\Phi}_a\big(\boldsymbol{x} - \boldsymbol{x}(\boldsymbol{X}_I, t)\big) \tag{10}$$

$$\dot{\Phi}_a\left(\frac{\|\boldsymbol{x} - \boldsymbol{x}(\boldsymbol{X}_I, t)\|}{a}\right) = \Phi_a^{'}\left(\frac{\|\boldsymbol{x} - \boldsymbol{x}(\boldsymbol{X}_I, t)\|}{a}\right)\frac{\boldsymbol{n}\cdot(\boldsymbol{v} - \boldsymbol{v}_I)}{a} \tag{11}$$

In (10), $\dot{\Phi}_a(\cdot)$ is the time derivative of the kernel function which takes into account the nodal transport effect in the semi-Lagrangian formulation.

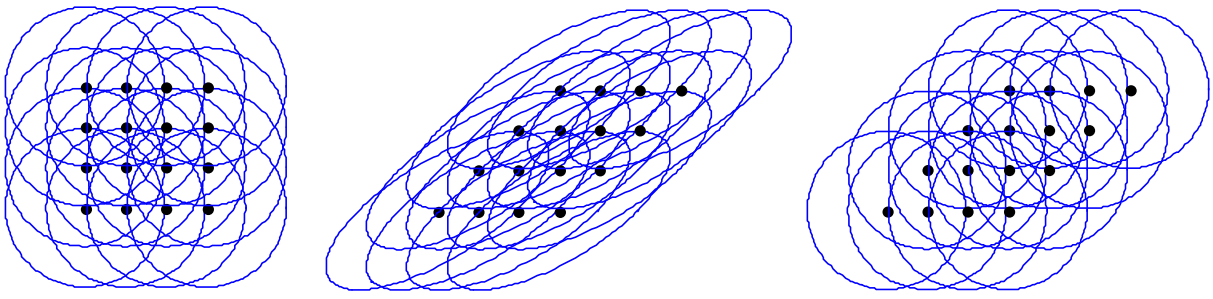

(a) **(b)** **(c)**

Figure 2. Nodal support definitions in a) initial configuration for Lagrangian or semi-Lagrangian formulation, b) Lagrangian formulation after deformation, c) semi-Lagrangian formulation after deformation

3 MICROCRACK-INFORMED DAMAGE MODEL

A microcrack informed damage model (MIDM) is proposed for describing the softening behavior of brittle solids, in which damage evolution is treated as a consequence of microcrack propagation [7]. The homogenized stress-strain relation in a cracked microscopic cell defines the degradation tensor, which can be obtained by the equivalence between averaged Helmholtz free energy (HFE) of the microscopic cell and HFE of the damaged continuum, $\overline{\Psi}$,as follows (with reference to Fig. 3).

$$\overline{\Psi} = \frac{1}{V_y}\left(\int_{\Omega_y} \Psi^{\varepsilon}\, d\Omega + \frac{1}{2}\oint_{\Gamma_c} \boldsymbol{u}^{\varepsilon}\cdot \boldsymbol{h}\, ds\right) \tag{12}$$

Here superscript "ε" is used for the fine scale variables, $\boldsymbol{u}^{\varepsilon}$ is the displacement field in the microscopic cell, $\boldsymbol{h}$ is the cohesive traction acting on the crack surface Γ_c, Ψ^{ε} is the HFE of the microscopic cell, and V_y is the volume of the microscopic cell with domain Ω_y . This energy equivalence relationship serves as an energy bridging vehicle between the damaged continuum and the cracked microstructure.

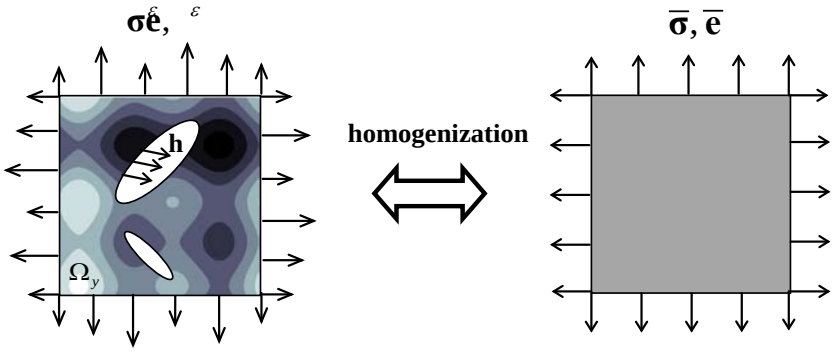

Figure 3. Homogenization of microscopic cell with fluctuating fields

By introducing bridging based on HFE, the damage tensor for the continuum can be obtained. Recall (12), and let $\overline{\Psi}$ computed from the microscopic cell be related to the damaged continuum by

$$\overline{\Psi} = \frac{1}{2}\bar{\boldsymbol{e}} : (\boldsymbol{I} - \boldsymbol{D}) : \overline{\boldsymbol{C}}_0 : \bar{\boldsymbol{e}} \tag{13}$$

where $\bar{\boldsymbol{e}}$, $\overline{\boldsymbol{C}}_0$, and **D** are the homogenized strain tensor, undamaged material response tensor, and the continuum damage tensor, respectively. The damage energy release rate is defined as

$$\boldsymbol{Y} = -\frac{\partial \overline{\Psi}}{\partial \boldsymbol{D}} = \frac{1}{2}\bar{\boldsymbol{e}} : \overline{\boldsymbol{C}}_0 : \bar{\boldsymbol{e}} \tag{14}$$

By taking the derivative of the HFE of the microscopic cell in (12) with respect to the damage energy release rate, **Y** , we obtain the damage tensor

$$\boldsymbol{D} = \boldsymbol{I} - \frac{\partial \overline{\Psi}}{\partial \boldsymbol{Y}} \approx \boldsymbol{I} - \frac{\Delta \overline{\Psi}}{\Delta \boldsymbol{Y}} \tag{15}$$

Here a finite difference approach could be used in (15) to obtain the fourth-order damage tensor using $\Delta\overline{\Psi}$ and $\Delta\mathbf{Y}$. This general approach can be reduced to scalar or bi-scalar damage models as discussed in [7].

4 IMPLEMENTATION

The MIDM was implemented into the Advanced Fundamental Concrete (AFC) model, developed by the U.S. Army ERDC [8]. The AFC model is a 3-invariant plasticity model which incorporates damage evolution, strain rate effects, and a nonlinear pressure-volume relationship. In the original AFC model, a single-scalar damage variable was used for failure surface evolution as a function of volumetric and effective deviatoric plastic strains. As an enhancement, in this work the damage variable was decomposed into two terms, one to consider damage in compression and another to consider damage in tension. The compression damage term, d_c, was calculated using the original AFC damage evolution equation. The tensile damage term, d_t, was calculated from the MIDM.

For use during implementation of the MIDM, an ultra high-strength, fiber-reinforced concrete known as CorTuf [9] was considered. CorTuf is reinforced with approximately 30-mm long, randomly distributed steel fibers, the effects of which were considered in the microscopic cell analysis.

4.1 Microscopic cell analysis

To determine the microcrack-informed tensile damage evolution function, the microscopic cell analysis was based on Mode I crack propagation in a center-cracked cell. Crack propagation in the cell was modeled using a cohesive crack model with a modified cohesive law. The conventional cohesive crack law applies cohesive stresses over a fracture processing zone near the crack tip, which extends from the so-called mathematical crack tip to the physical tip. The cohesive law is then expressed as the relationship between cohesive stresses and crack opening displacement (COD), and the area under the resulting curve is equal to the fracture energy, G, of the material. The modified cohesive law was formulated to consider the effect of fiber bridging in CorTuf, such that cohesive stresses extend beyond the typical fracture processing zone. Based on a Griffith-type crack formation, the cohesive stress versus COD relationship was assumed to consist of a constant stress region which represents fiber bridging effects and a softening region which corresponds to a region of fiber failure. Fracture energy of the modified law was equivalent to experimentally determined values.

Solving the microscopic cell problem by RKPM, the average microscopic cell strain, stress, and HFE were determined. Utilizing the microscopic cell results in conjunction with the homogenization relationships in Section 3, the tensile damage parameter versus homogenized continuum strain relationship was determined, as shown in Figure 4. Here nonlinearity of the microcrack-informed tensile damage evolution function is noted.

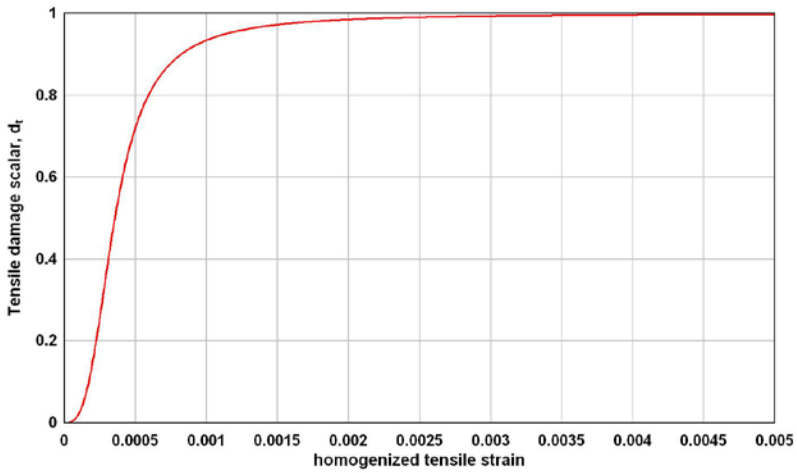

Figure 4. Microcrack-informed tensile damage evolution function for CorTuf concrete

Evolution of the AFC model yield surfaces with and without the microcrack-informed tensile damage function are shown in Figure 5. Sign convention is adopted such that $(+)I_1$ indicates compression and $(-)I_1$ indicates tension. From Figure 5a, it is seen that when a single scalar damage term is used, the tension and compression yield surfaces contract together with damage evolution. However, from Figure 5b it is observed that when the damage variables are separated, the tensile yield surface may evolve independently of the compression yield surface.

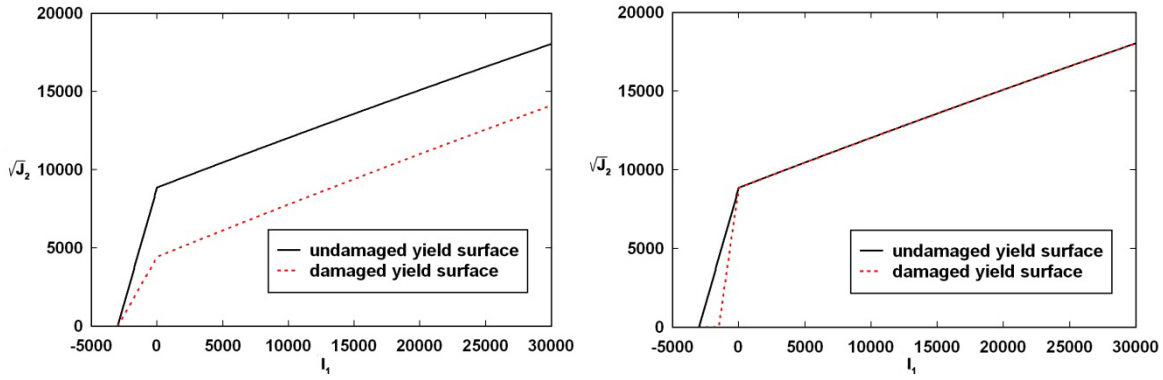

Figure 5. AFC model yield surface with a) compression damage only (d_c=0.5) b) separated tension and compression damage (d_c=0, d_t=0.5); (I_1=first stress invariant, J_2=second deviatoric stress invariant)

5 BENCHMARK PROBLEM

The multiscale RKPM formulation for penetration and impact was implemented into the *Nonlinear Meshfree Analysis Program* (*NMAP*) parallel code [10], which was used to analyze a series of benchmark penetration problems. The benchmark problems followed penetration experiments performed by ERDC in their small-caliber ballistic test facility [11]. The experiments were conducted by firing spherical projectiles (S2 tool steel) into thin-panel CorTuf targets where impact velocity, projectile size and panel thickness were varied to achieve a range of terminal ballistic conditions. Results from one of these experiments are presented here, where an 11-mm diameter projectile with a mass of 86 grains was fired into an approximately 25-mm-thick panel. Impact velocity of the projectile was 538 m/s. The projectile exited the panel's back face, but with insufficient velocity to reach the exit-face-velocity measuring devices.

For the *NMAP* model, the projectile and panel were discretized using 1,163 nodes and 190,000 nodes, respectively. This provided a nodal spacing of approximately 1 mm on the surface of the projectile and 1.4 mm in the impact region of the panel. The projectile was modeled using a J2 plasticity model with isotropic hardening, with material model parameters as given in Table 1. The CorTuf target was modeled using both the original AFC model and the MIDM-enhanced formulation.

parameter	value
Young's modulus, E	200 GPa
Poisson's ratio, ν	0.26
yield stress, σ_y	2400 MPa
hardening modulus, H	2500 MPa
density	7806 kg/m^3

Table 1. J2 plasticity model parameters for projectile

Snapshots from the penetration process are shown in Figure 6. Notable is the debris generated from the exit face. Because each "flying" node contains velocity and mass data, this can be directly translated to momentum and energy of debris generated from the impact event.

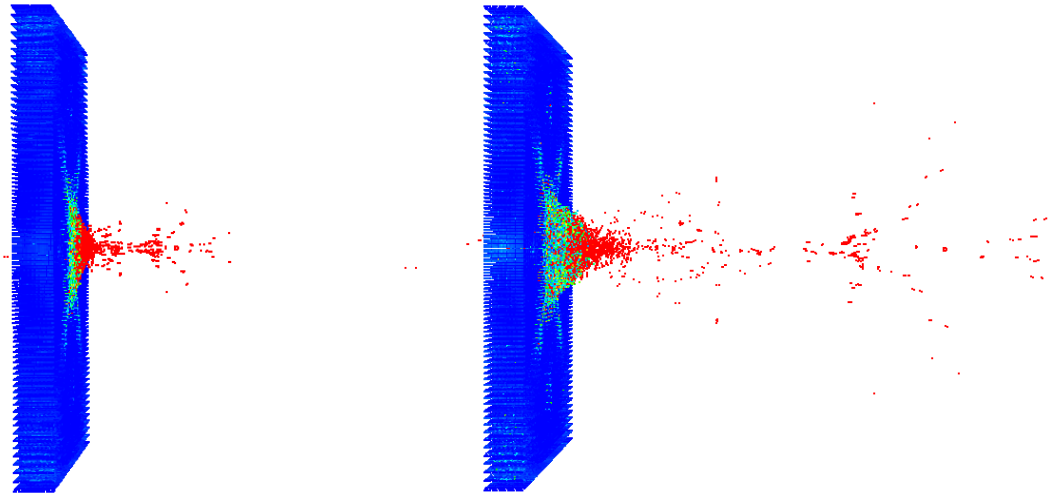

(a) **(b)**

Figure 6. Penetration process using MIDM-enhanced AFC formulation a) 300 μsec after impact, b) 1000 μsec after impact.

Exit velocity, velocity reduction, and mass loss of the projectile are compared in Table 2. As seen from the data, both sets of numerical results are in excellent agreement with the experimental data. The MIDM-enhanced formulation predicted a marginally higher exit velocity than the original AFC formulation, but both solutions were within approximately 0.3 percent of the experimental results. In terms of projectile mass loss, both models slightly under predicted the experimental result. This is due to the fact that damage was not included in the projectile material model. However, as with the exit velocities, the numerically predicted projectile mass loss is still in good agreement with the experimental results.

	impact velocity, m/s	exit velocity, m/s	velocity reduction, %	projectile mass loss, %
experiment	538	~0	~100	0.2
original AFC	538	1.2	99.8	0
MIDM-enhanced AFC	538	1.7	99.7	0

Table 2. Comparison of results

Experimental and numerical damage patterns on the panel faces are compared in Figure 7. Simulation data are shown for the MIDM-enhanced model, where edges of the experimentally measured craters are shown in black. As seen, the calculated zones of heavy damage generally matched the crater limits, with some additional damage extending beyond. Extension of panel damage beyond the crater limits is commonly observed in this type of penetration experiments, indicating generally good agreement between the experimental and numerical results. Notably, damage zones calculated without the multiscale enhancement were smaller, and did not appear to capture the panel damage as well.

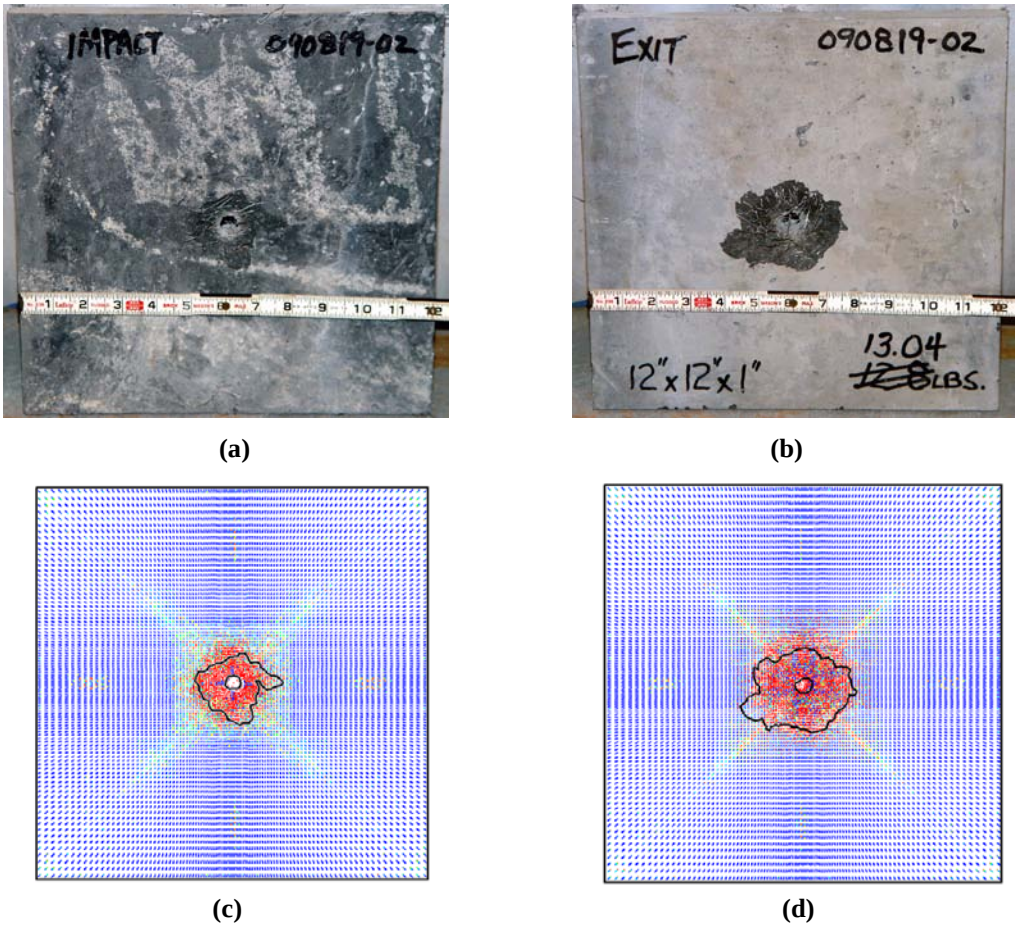

(a) **(b)**

(c) **(d)**

Figure 7. Comparison of experimental and numerical damage patterns (tensile damage parameter plotted). a) experimental impact face, b) experimental exit face, c) numerical impact face, d) numerical exit face.

6 CONCLUSIONS

In this research an RKPM formulation was developed for penetration modeling, which was successfully used to model the penetration of ultra high-strength concrete targets. From the benchmark problem, it was seen that due to the reduced mesh-dependency of RKPM, large-scale material failure and separation was captured without problem. This implies that the method not only has capability to accurately model terminal ballistic effects within the target, but can also accurately capture secondary effects such as behind-target debris – which is of great interest in certain applications.

A multiscale model for damage evolution in ultra high-strength concrete was also developed and implemented into the RKPM-based *NMAP* code. The basic approach was to utilize a microscale calculation to determine constitutive model parameters (in this case the damage evolution function) which otherwise would be phenomenologically determined. Therefore, in essence the microscopic cell analysis serves as a microscale numerical experiment, where microcrack propagation within the material can be modeled explicitly. Scale bridging is used to link the microscale cracking to continuum-scale damage evolution, and as a result damage evolution in the continuum is based on a more fundamental aspect of material response. A novel energy-bridging method was also developed for scale bridging, which provides a more computationally efficient link between the micro- and macroscales. Note that for the example given, the multiscale model was used to define tensile damage evolution, and therefore the microscopic cell analysis only considered Mode I crack

propagation. However, more complex conditions within the microscopic cell could also be addressed under this multiscale modeling framework. This is a topic of ongoing research within the program.

From results of the benchmark problem, it was seen that both the original AFC model and the MIDM-enhanced model were in excellent agreement with the experimentally measured exit velocity. The MIDM-enhanced AFC model also provided a very good prediction of panel damage on both the impact and exit faces, while the original AFC model tended to predict smaller damage areas.

ACKNOWLEDGEMENT

Permission to publish was granted by Director, Geotechnical and Structures Laboratory. Simulations were partly performed on the Department of Defense Super Computing Resource Center high performance computers.

REFERENCES

[1] I. Rohr, H. Nahme, K. Thoma, Material characterization and constitutive modelling of ductile high strength steel for a wide range of strain rates, *International Journal of Impact Engineering*, **31**, 401-433, 2005.

[2] J.S. Chen, C. Pan, C.T. Wu, and W.K. Liu, Reproducing kernel particle methods for large deformation analysis of nonlinear structures, *Computer Methods in Applied Mechanics and Engineering*, **139**, 49-74, 1996.

[3] W.K. Liu, S. Jun, and Y.F. Zhang, Reproducing kernel particle methods, *International Journal for Numerical Methods in Fluids*, **20**, 1081-1106, 1995.

[4] J.S. Chen, C. Pan, C. Roque, and H.P. Wang, A Lagrangian reproducing kernel particle method for metal forming analysis, *Computational Mechanics*, **22**, 289-307, 1998.

[5] P. Guan, J.S. Chen, Y. Wu, H. Teng, J. Gaidos, Hofstetter, K, and M. Alsaleh, A semi-Lagrangian reproducing kernel formulation for modelling earth moving operations, *Mechanics of Materials*, **41**, 670-683, 2009.

[6] P.C. Guan, S.W. Chi, J.S. Chen, T.R. Slawson, and M.J. Roth, Semi-Lagrangian reproducing kernel particle method for fragment-impact problems, *International Journal of Impact Engineering*, submitted.

[7] X. Ren, J.S. Chen, J. Li, T.R. Slawson, M.J. Roth, Micro-cracks informed damage model for brittle solids, *International Journal for Solids and Structures*, accepted, 2011.

[8] Adley, M.D., Frank, A.O., Danielson, K.T., Akers, S.A., O'Daniel, J.L., The Advanced Fundamental Concrete (AFC) Model, *Technical Report ERDC/GSL TR-11-xx (in publication)*, U.S. Army Engineer Research and Development Center, Vicksburg, MS.

[9] Williams, E.M., Graham, S.S., Reed, P.A., and Rushing, T.S., Laboratory Characterization of Cor-Tuf Concrete With and Without Steel Fibers, *Technical Report ERDC/GSL TR-09-22*, U.S. Army Engineer Research and Development Center, Vicksburg, MS.

[10] Roth, M.J., Chen, J.S., Slawson, T.R., Chi, S.W., and Lee, C.H., User's Manual for Nonlinear Meshfree Analysis Program (NMAP), Version 1.0, *Technical Report ERDC/GSL TR-11-xx (in publication)*, U.S. Army Engineer Research and Development Center, Vicksburg, MS.

[11] Boone, R.N., Ballistic Impact and Perforation of Ultra-high Strength Concrete Panels, *M.S. thesis (in preparation)*, Mississippi State University.